Recent advances on electrochemical sensors for the detection of organic disinfection by-products in water

Wei Zhang[1], Lue Wang[1], Yuesuo Yang[2], Paul Gaskin[3] and Kar Seng Teng[1]

1. *College of Engineering, Swansea University, Bay Campus, Swansea SA1 8EN, UK*
2. *College of Environment and Recourses, Jilin University, Changchun 130012, China*
3. *Dŵr Cymru Welsh Water, Newport, NP10 8FZ, UK*

Abstract

Irreversible organ damage or even death frequently occurs when humans or animals unconsciously drink contaminated water. Therefore, in many countries drinking water is disinfected to ensure harmful pathogens are removed from drinking water. If upstream water treatment prior to disinfection is not adequate, disinfection by-products (DBPs) can be formed. DBPs can exist as wide variety of compounds, but up till now, only several typical compounds have drinking water standards attributed to them. However, it is apparent that the range of DBPs present in water can comprise of hundreds of compounds, some of which are at high enough concentrations that can be toxic or potentially carcinogenic. Hence, it becomes increasingly significant and urgent to develop an accessible, affordable and durable sensing platform for a broader range and more sensitive detection of DBPs. Compared with well-established laboratory detection techniques, electrochemical sensing has been identified as a promising alternative that will provide rapid, affordable and sensitive DBPs monitoring in remote water sources. Therefore, this article provides a review on current state-of-the-art development (within last decade) in electrochemical sensing to detect organic DBPs in water, which covered three major aspects: (1) recognition mechanism, (2) electrodes with signal amplification, and (3) signal read-out techniques. Moreover, comprehensive quality assessments on electrochemical biosensors, including linear detection range, limit of detection (LoD) and recovery, have also been summarized.

Keywords: Electrochemical; Sensors; Disinfection by-products; Haloacetic Acids; Trihalomethanes; Nitrosamines; Water quality; Water monitoring.

Water is indispensable for all life on earth. The security of drinking water is vital to public health and the quality of life in any community or country [1]. Modern disinfection process forms an essential part of municipal water treatments for the control of waterborne pathogens[2]. However, the highly reactive nature of disinfectant (e.g. chlorine, chlorine dioxide, chloramines or ozone) can interact with natural organic matters or anthropogenic pollutants (e.g. halogenated solvents, pharmaceuticals or pesticides) in water sources and produce a number of secondary organic contaminants or DBPs[3]. Until recently, the well-known adverse health effects (e.g. possible human carcinogen) have led to establishment of guideline values for some of those organic DBPs in drinking water by WHO (see Table 1)[4]. Traditional water treatments such as coagulation and filtration before the disinfection process could reduce the DBPs formation by lowering the level of natural organic matter, however, their effectiveness in terms of meeting the drinking water regulation can be limited depending on the nature of the organics involved and their respective removal rates. There has been a constant increase in new member of DBPs, and the organic DBP family has expanded as many as 700 variants identified in drinking water so far[5]. Among those, trihaomethanes and haloacetic acids, and nitrosamines are three major groups of greatest health concern and are closely monitored by various environment agencies in most countries. Accordingly, this review only discusses the current state-of-the-art detection techniques for these three major groups of organic DBPs. A more systematic classification of DBPs can be referred to a review contributed by Richardson et al[6].

Haloacetic Acids in Water

Haloacetic acids (HAAs) are a class of DBPs that are often produced from the interaction between certain disinfectant (e.g. chlorine) and pollutants (e.g. NOMs, chlorate and bromide) during the process of water disinfection. Compared with fluorinated or iodinated analogs, brominated and chlorinated HAAs present higher ubiquity as up to nine variants have already been systemically classified and denoted as HAA9[7]. High health risks to human beings either transient or chronic exposure to HAAs lead to necessary regulations of maximum permissible concentrations issued by many organizations[8]. The United States Environmental Protection Agency (U.S. EPA) recently claimed a Stage 2 Disinfectants and Disinfection Byproducts Rules for a total maximum contaminant level HAA as of 60 μg/L[9].

HAA5 consists of monochloroacetic acid (MCA), monobromoacetic acid (MBA), dichloroacetic acid (DCA), dibromoacetic acid (DBA) and trichloroacetic acid (TCA). Trichloroacetic acid (TCA, MW 163.38 g/mol, CCl_3COOH) is an organic halide that has been regarded as one of the main environmental concerns as a by-product of water chlorination[10]. Due to its high solubility in water, it is severely harmful to humans as well as other living creatures with potential carcinogenic (e.g. liver, renal and intestinal tumors[11]) and mutagenic effects[12] even at very low concentrations. In addition to water chlorination, TCA may be introduced into aquatic environment via other anthropogenic activities, such as industrial laundry work[13], agricultural routines (e.g. pesticides and herbicides spraying[14]) and usage of peeling agent especially for tattoos or impaired skin[15]. Dibromoacetic acid (DBA, MW 217.84 g/mol, $CHBr_2COOH$) is another typical halogenated DBP that exhibits not only carcinogenicity but also more potent reproductive toxicity (e.g. spermatotoxicity) compared with dichloroacetic acid (DCA, MW 128.94 g/mol, $CHCl_2COOH$)[16]. Moser et al. found DBA also presented concentration-related neuromuscular toxicity to the rats through a long-term DBA exposure in the drinking water and suggested the neurotoxicity should receive more attention in the whole hazard assessment of HAAs[17].

Tribromoacetic acid (TBA, MW 296.74 g/mol, CBr_3COOH) is an analogue of TCA in which all the three hydrogen atoms are replaced by bromine atoms. Normally, TBA is coupled with other two brominated trihaloacetic acids, bromodichloroacetic acid (BDCA, MW 207.83 g/mol, $CBrCl_2COOH$) and dibromochloroacetic acid (DBCA, MW 252.29 g/mol, $CBr_2ClCOOH$) to constitute the HAA3 group. It has

been demonstrated that HAA3 is much less prevalent than HAA5, however they are more fetotoxic, genotoxic and cytotoxic in mammalian cells[18,19,20].

Trihalomethanes in Water

Trihalomethanes (THMs) are another main group of organic DBPs, including trichloromethane, bromodichloromethane, dibromochloromethane and tribromomethane. They are frequently formed when chlorine-related disinfectant reacts with natural organic compounds (e.g. humic acid) or inorganic species (e.g. chlorate and bromide) in the water[21]. Like HAAs, THMs also exhibit high toxicity, mutagenicity, carcinogenicity and fetotoxicity (or teratogenicity) to the humans[22,23]. The MCL for total trihalomethane in drinking water was established by the U.S. EPA based on the protocol "Stage 2 Disinfectants and Disinfection Byproducts Rules" as of 80 μg/L[20].

Trichloromethane or chloroform (TCM, MW 119.37 g/mol, $CHCl_3$) is a colorless organic solvent with special odor. It is the most volatile trihalomethane often detected from soil and surface water due to the high emission generated by fungi and seaweeds, respectively[24]. Chloroform has been widely used as a precursor to refrigerants (e.g. Freon), medical grade anaesthetic or fundamental solvent in laboratory. The mouse bioassay study showed the toxicity with LD_{50} values of 908 mg/kg for male rats and 1117 mg/kg for the female[25]. Bromodichloromethane (BDCM, MW 163.82 g/mol, $CHBrCl_2$) is another halohydrocarbon which can cause an irreversible damage to living bodies mainly through ingestion, inhalation and skin penetration. The toxicity of BDCM is slightly higher than that of chloroform with LD_{50} values of 916 mg/kg for male rats and 969 mg/kg for the female[25]. Dibromochloromethane (DBCM, MW 208.28 g/mol, $CHBr_2Cl$) is recognized as a further brominated BDCM. Small amount of DBCM is produced in ocean by algae. With an increase of molecular weight (e.g. more bromine atoms occurring), the corresponding THMs become heavier and less flammable[26]. Therefore, both BDCM and DBCM can be utilized as flame retardants. LD_{50} for DBCM are 1186 mg/kg for male rats and 848 mg/kg for the female[25]. Tribromomethane or bromoform (TBM, MW 252.73 g/mol, $CHBr_3$) is an analogue of chloroform. Bromoform can be naturally generated by phytoplankton and seaweeds in the ocean[27], however, this amount is not comparable with the yields of water chlorination. LD_{50} with respect to bromoform are 1388 mg/kg for male rats and 1147 mg/kg for the female[25].

Nitrosamines in Water

In many countries, chloramines have been gradually adopted as an alternative disinfectant to chlorine to reduce the formation of THM and HAA[28]. However, this practice has shifted attention to an emerging group of DBPs, such as nitrosamines[29,30]. The family of nitrosamines consist of five basic individuals including *N*-nitrosodimethylamine, *N*-nitrosopyrrolidine, *N*-nitrosomorpholine, *N*-nitrosopiperidine and *N*-nitrosodiphenylamine[31]. In particular, *N*-nitrosodimethylamine (NDMA, MW 74.08 g/mol, $(CH_3)_2N_2O$) has been shown to be far more toxic than the traditionally regulated classes of DBPs (e.g. HAAs and THMs)[32]. In comparison to other DBPs, mouse acute toxicity study showed a much lower LD_{50} for NDMA ranging from 23 to 40 mg/kg[33]. It has been classified as "probably carcinogenic to humans" by the International Agency for Research on Cancer[34]. Based on an upper-bound excess lifetime cancer risk of 10^{-5}, a guideline value for NDMA in drinking water of 100 ng/L has been included in the latest Guidelines for Drinking-Water Quality by WHO (2011). Since then, more EU countries have begun to regulate their presence in drinking water. In Germany, for instance, 10 ng/L concentrations would trigger the initiation of remedial actions to reduce NDMA concentrations.

Current Standard Methods for the Detection of Organic DBPs in Water

Most of these three major groups of organic DBPs can be chronically accumulated in the living bodies normally through ingestion (e.g. drinking water)[35], which can increase the risk of cancer while some of them

even present high genotoxicity. Their concentrations are affected by various factors, leading to regional difference from a trace amount of ng/L to μg/L with some rare exceptions of several hundreds or thousands of μg/L. For instance, a great amount of *N*-nitrosodimethylamine (up to 400 μg/L) was detected from groundwater in the areas adjacent to rocket engine testing facilities, California. This was probably caused by the microbiological conversion of the unsymmetrical dimethylhydrazine (UDMH)-based rocket fuels[34]. The current laboratory-based technique for these three major groups of DBPs assessment is a two-step process of solid phase extraction and gas chromatography coupled with mass spectrometer (GC-MS) or electron capture detector (GC-ECD), which proves to be time-consuming, complex and expensive. Therefore, it is impractical to produce guideline values for many and especially emerging organic DBPs identified in drinking water now since sensitive and cost-effective monitoring is lacking. Fast *in situ* and highly sensitive detection methods including multiplexing capability are urgently needed to ensure that current and future regulations are upheld for current and emerging organic DBPs without impacting on disinfection effectiveness.

Table 1 Current WHO drinking water guideline values and adopted detection methods for organic DBPs[4]

DBPs	Limit of detection	Guideline values
Trichloroacetic acid	6.12 nM by GC-MS or GC-ECD	1.22 μM
Chloroform	0.54–1.08 nM by purge-and-trap and liquid–liquid extraction and direct aqueous injection in combination with a chromatographic system; 0.54 nM by GC-ECD; 11.83 nM by GC-MS	2.51 μM
Bromoform		0.39 μM
Dibromochloromethane		0.48 μM
Bromodichloromethane		0.36 μM
N-Nitrosodimethylamine	0.37 pM by capillary column GC and chemical ionization tandem MS; 5.4 pM by capillary column GC and high-resolution MS; 9.4–21.6 pM by GC-MS and ammonia positive chemical ionization detection	1.35 nM

Analytes	Electrode substrates	Signal amplification strategies	Electrode binders	Recognition molecules	Film forming agents	Linear ranges (LoD)
TCA	GCE	SWNTs	[BMIM][PF_6]	Hematin	-	0.9 to 140µM (0.38µM)
TCA	GCE	TNTs	-	Thionine	Chitosan	15 to 1500µM (-)
TCA	GCE	AgNPs	-	-	Chitosan	3 to 56µM (1.1µM)
TCA	CILE	GR/AgNPs	$BPPF_6$	Hb	Chitosan	0.8 to 22mM (0.42mM)
TCA	CILE	GR	$EMIMBF_4$	Mb	Chitosan	2 to 16mM (0.583mM)
TCA	CILE	GR/dsDNA	PPBF4	HRP	Nafion	1 to 21mM (0.133mM)
TCA	GCE	MWCNTs	-	Phtalocyanine	-	0.008 to 20mM (2.0µM)
TCA	CPE	CdO	-	-	-	3 to 230µM (2.3µM)
TCA	CILE	GR/TiO_2 nanorods	$BPPF_6$	Hb	Nafion	0.6 to 21mM (0.22mM)
TCA	CILE	GR/MWCNTs	$HPPF_6$	Hb	Nafion	0.05 to 38mM (0.015mM)
TCA	CILE	GR/Mg_2Al LDH	$HPPF_6$	Hb	Chitosan	1.6 to 25mM (0.534mM)
TCA	CILE	GR/AuNP	$HPPF_6$	Mb	Nafion	0.4 to 20mM (0.13mM)
TCA	CILE	GR/Pt	BPPF6	Mb	Nafion	0.9 to 9mM (0.32mM)
TCA	Gold electrode	RGO	-	MIPs	-	0.5 to 100ppb (-)
TCA	CILE	N-doped GR	$HPPF_6$	Hb	Chitosan	0.2 to 30mM (0.13mM)
TCA	CILE	GR/NiO	$HPPF_6$	Mb	Nafion	0.69 to 30mM (0.23mM)
TCA	CILE	3D-GR	HPPF6	Hb	Chitosan	0.4 to 26mM (0.133mM)
TCA	CILE	GR/CuS	BPPF6	Hb	Chitosan	3.0 to 64mM (0.2mM)
TCA	CILE	GR/exfoliated Co_2Al LDH	BPPF6	Hb	Chitosan	2.5 to 360mM (0.82mM)
TCA	CILE	3D-RGO/Au	HPPF6	Mb	Chitosan	0.2 to 36mM (0.06mM)
TCA	CILE	GR	HPPF6	Mb	Chitosan	0.6 to 26mM (0.15mM)
TCA	CILE	GR/ZrO_2	HPPF6	Mb	Chitosan	0.4 to 29mM (0.13mM)
TCA	CILE	GR/Bi	HPPF6	Mb	Nafion	0.5 to 46mM (0.167mM)
TCA	CILE	GR/ Fe_3O_4	-	Mb	SA/Nafion	1.4 to 119.4mM (0.174mM)
TCA	CILE	GR/ Co_3O_4	[BMIM]BF_4	Mb	Chitosan	1 to 20mM (0.18mM)
TCA	GCE	Core-shell Au@Ag nanorods	-	Hb	PSS/PDDA	0.16 to 1.7µM (0.12µM)

TCA	CILE	GR/ Pd	$HPPF_6$	Hb	Nafion	0.6 to 61mM (0.35mM)
TCA	CILE	GR/NiO/[EMIM]EtOSO$_3$	[EMIM]BF4	Hb	Nafion	1.5 to 10mM (0.5mM)
TCA	CILE	GR/ SnO_2	$[BMIM]BF_4$	Hb	Nafion	2 to 11mM (0.615mM)
TCA	CILE	GR	-	Mb	SA/Nafion	7.5 to 69mM (0.163mM)
TCA	CILE	GR-COOH	HPPF6	Mb	Nafion	5 to 57mM (1mM)
TCA	CILE	3D-GR/ ZnO	HPPF6	Mb	Nafion	0.5 to 30mM (0.167mM)
TCA	CILE	GR/Co_3O_4	HPPF6	HRP	Nafion	1 to 53mM (0.33mM)
TCA	CILE	CdS/ $[EMIM]EtOSO_3$	([BMIM]BF4)	HRP	HA	1.6 to 18mM (0.53mM)
BDCA, DBCA and TBA	Gold electrode	-	-	-	-	50 to 1200µg/L (-)
DBAA and TBM	Gold electrode	DWCNTs	-	-	PDMS	1ppt to 1ppm (0.01ppt)
TCA	GCE	AgNPs/ MA	-	-	-	0.1 to 100µM (30nM)
TCA	CILE	Boron-doped GQDs	HPPF6	Hb	Nafion	0.1 to 300mM (0.053mM)
TCA	CILE	GR/g-C_3N_4/Co_2Al LDH	BPPF6	Hb	Chitosan	0.2 to 36mM (0.05mM)
Bromoform and Chloroform	Silver electrode	-	-	-	-	- (12nM for Bromoform, 50nM for Chloroform)
NDMA	GCE	-	-	MIPs	-	10 to 230µg/L (0.85µg/L)

Table 2 A summary of detection results of organic DBPs using various electrochemical sensors in literature

DBPs DETECTION USING ELECTROCHEMICAL BIOSENSORS

Electrochemical biosensors have been of great research interest in environmental monitoring owing to its rapid response, excellent sensitivity, affordability and potential portability[77,78,79]. Based on previously published work, successful electrochemical biosensing of DBPs in drinking water was generally dependant on three main aspects: 1) Recognition molecules, 2) electrodes and their modifications, and 3) signal read-out techniques[80].

Recognition molecules. Superior sensitivity and specificity of electrochemical sensors can only be achieved when there are well-covered recognition molecules or labels as bridges for electron transfer between electrodes and target molecules. Up to date, redox proteins such as hemoglobin (Hb) (**Figure 1a**)[39,43,44,45,46,50,52,53,54,61,62,63,64,73,74] and myoglobin (Mb)[40,47,48,51,55,56,57,58,59,60,65,66,67], metal complexes including porphyrin[36] (**Figure 1b**), enzymes like horseradish peroxidase (HRP)[41,68] and phthalocyanine[42], and molecular imprinted polymers (MIPs)[49,76] (**Figure 1c**) have been applied as recognition molecules for electrochemical determination of various DBPs in water. From **Table 2** (28 out of 40 literatures), the application of redox proteins was of particular dominant as compared with other recognition mechanism. Myoglobin (Mb, MW 17800 Da) is a globule-structured monomeric protein that consists of 153 amino residues with a heme group (e.g. Fe^{III}/Fe^{II}) which has the responsibilities in carrying oxygen molecules to muscle tissues in most of mammals. Hemoglobin (Hb, MW 64500 Da) is another common redox protein of a molecular weight larger than Mb. Hb is generally made up of four helical amino acid chains (e.g. two α and two β), which are always cross-linked with each other to form a complicated spherical microenvironment for heme iron-decorated porphyrin[81]. The biological function of Hb is similar to that of Mb, which is responsible for oxygen storage and transportation especially in red blood cells. With a reputation of strong electrocatalytic activity on various analytes (e.g. TCA), redox proteins have been increasingly reported in the application of electrochemical biosensing[82]. However, the electroactive centres (e.g. ferric-ferrous porphyrin) were usually deeply shielded by polypeptide chains, leading to a relatively poor sensitivity and selectivity (e.g. detection ranges and LoDs were limited only in the range of mM) of these biosensors. Instead of using redox couple-protein assembly, some studies simplified the recognition approach by only introducing basic metal complex components of Mb and Hb structures to the sensor electrodes, such as porphyrin and phthalocyanine. This strategy could mimic the same function of large redox proteins (i.e. binding of redox ferric-ferrous species in solution) but provide much improved sensitivity and long-term storage stability. For example, hydroxyferriprotoporphyrin (hematin)[36], a mimic of hemeprotein, and phtalocyanine[42] was demonstrated to dechlorinate TCA to acetic acid efficiently with wider detection range and lower LoD than those of previously reported Mb and Hb enabled electrochemical sensors.

Enzymes are recognized as highly-selective biological catalysts that can dramatically reduce a specific biochemical process by lowering the threshold of activation energy. For example, horseradish peroxidase (HRP, MW 40000 Da) derived from the roots of horseradish[83], has been applied in the fabrication of electrochemical biosensors by detecting reduction current of TCA in solution[41,68]. It should be noted that ambient environment (e.g. temperature and pH) is highly essential for enzymes as unsuitable conditions would lead to protein denaturing or even inactivation. On the other hand, the need for an extra step of acidity adjustment (e.g. in case of HRP, pH 3 is essential) may also reduce the practicality of this type of biosensors.

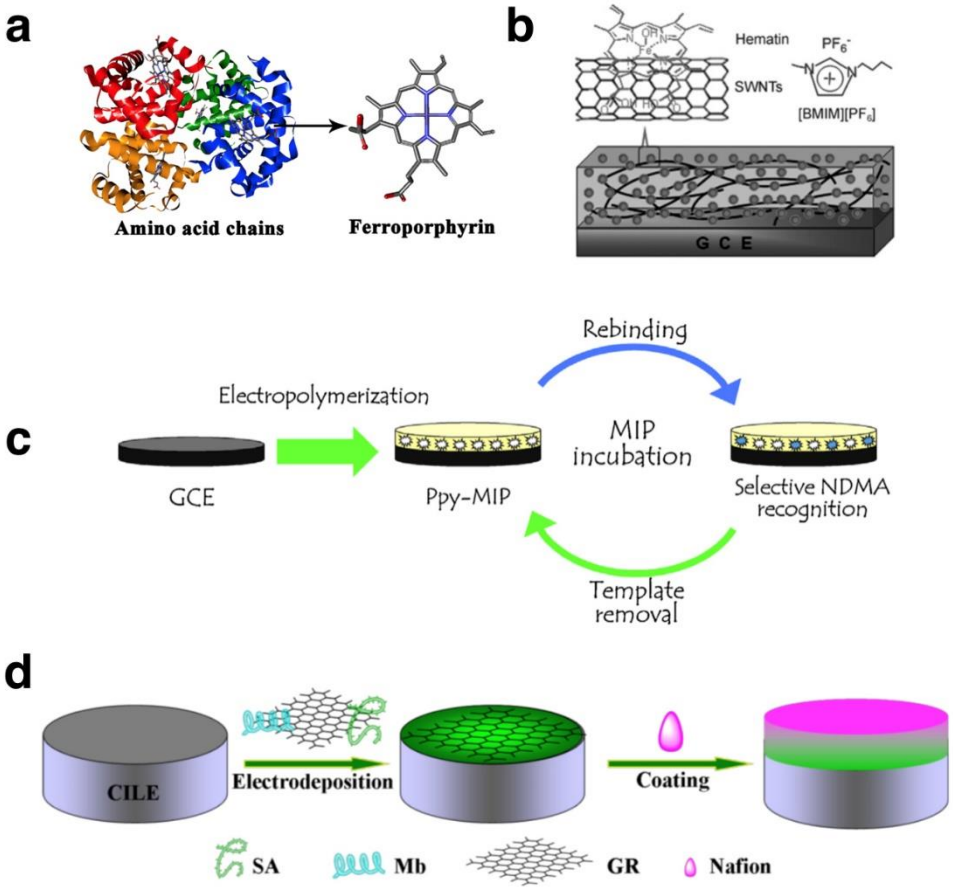

Figure 1. Different recognition mechanism for DBPs detection in water: a. 3D-structure of hemoglobin (Hb) and ferroporphyrin as bioactive center (Reproduced with permission of ref 73, Copyright 2018 Elsevier), b. hydroxyferriprotoporphyrin (hematin) immobilized on the SWNTs (Reproduced with permission of ref 36, Copyright 2009 Wiley), c. MIP sensor for the detection of NDMA (Reproduced with permission of ref 76, Copyright 2016 Elsevier), d. Nafion/Mb-SA-GR-CILE (Reproduced with permission from ref 65, Copyright 2017 ESG).

To prevent recognition molecules (e.g. redox proteins and enzymes) from damage and leakage during sensor fabrication process, many film forming agents including chitosan[37,38,39,40,46,50,52,53,54,55,56,57,60,74] and Nafion[41,44,45,47,48,51,58,59,62,63,64,65,66,67,68,73] were utilized to form a durable electrochemical sensing matrix. The activity of biomolecules was maintained due to the presence of microenvironments built by these film forming agents[84]. Zhu et al. implemented hyulanonic acid (HA) as the biocompatible film forming material in an electrochemical biosensor for TCA detection[69]. Sodium alginate (SA), a natural occurring polymer with abundant of carboxyl groups, has become another promising film forming agent since the alginate acid gels can form at the anode owing to the decrease of pH[59,85,86]. Utilizing this property, Chen et al. demonstrated an electrochemical biosensing interface for accurate determination of TCA by applying SA and Nafion to provide a dual fixation effect on Mb[64]. A schematic diagram for this electrochemical biosensor is shown in **Figure 1d**.

Aforementioned recognition molecules including redox proteins, metal complexes and enzymes are all commercially available, however, at very high production cost. Generally, biosensing platforms using these recognition molecules are likely to suffer from potential redox cycling, leading to an inevitable analyte transformation. In addition, no selectivity assessment against other similar DBP variants was carried out in all the reported studies, which seriously affect the practical application of these biosensors since simultaneous generation of multiple DBP analogues are commonly detected during any

disinfection process. In recent decades, the use of molecular imprinting technique in electrochemical biosensing has been increasing due to high selectivity, long shelf life, low cost and facile detection procedure[87]. Molecular imprinted polymers (MIP) belong to a novel group of synthetic bioreceptors with specially manufactured microcavities showing high affinity and specificity for any given analyte molecule[88]. Firstly, functional monomers, cross linking agent and template molecule (i.e. analyte) were simultaneously introduced together to form a template solution, followed by drying and crushing to yield MIPs fine particles (see **Figure 2**). MIP fine particles were then introduced to polymer matrix for a robust entrapment through either covalent or non-covalent interaction on top of substrate (i.e. electrode surface). The tailored bioreceptor sites (microcavities) were eventually revealed after the removal of template analyte and thus could selectively rebind with target analyte. Based on an MIP method (using 4-vinyl pyridine as monomer, ethylene glycol dimethyl acrylate as cross linker, and polysulphone as polymer matrix), Kibechu et al. developed a chemo sensor comprising of gold electrode modified with reduced graphene oxide (RGO) for the detection of TCA in aqueous solution. Template molecule elimination in their work was achieved by continuous washing step indicating that non-covalent conjugation was probably more appropriate method without any extra requirement of other reagents or operations to break the covalent bonds[49]. Cetó et al. demonstrated a MIP method using methacrylic acid as functional monomer and electropolymerized pyrrole as entrapment matrix for a successful electrochemical detection of NDMA in water[76]. The electrochemical performances (e.g. range of detection and LoD) and more importantly selectivity against other DBP analogues were much improved by these MIP-based biosensors implying a promising route for in-situ detection of DBPs.

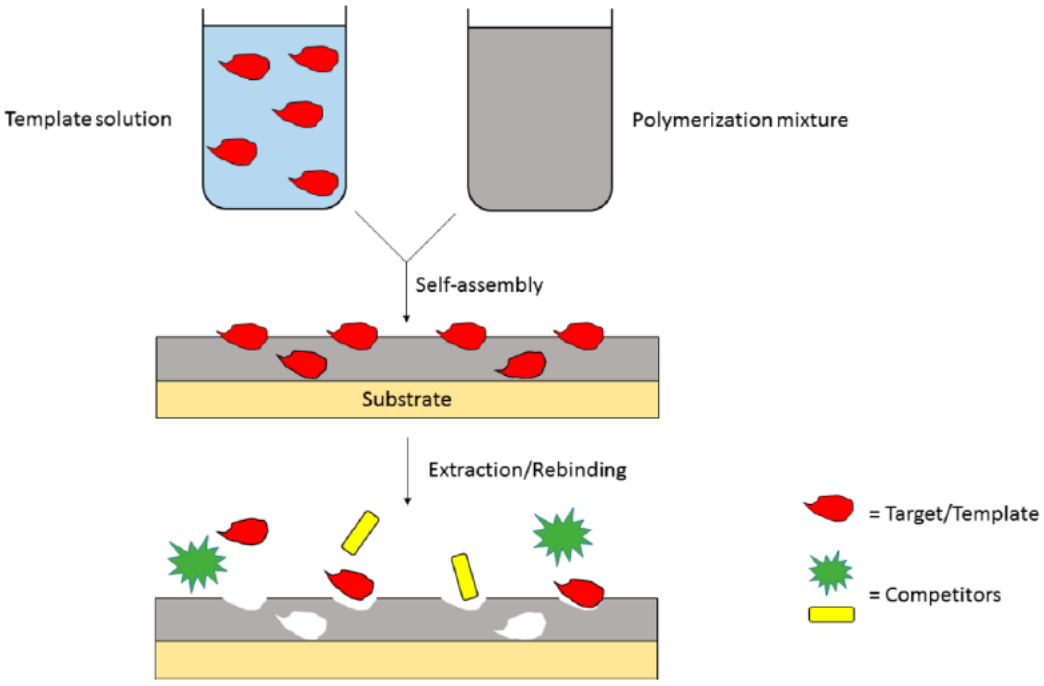

Figure 2. Scheme of the self-assembly technique for MIP synthesis. The template is mixed with the polymerization mixture containing monomers, cross-linker(s), and initiators. The MIP forms through interaction of the template with monomers during polymerization. After template extraction, microcavities on the MIP surface are able to rebind targets selectively (Reproduced with permission of ref 89, Copyright 2016 American Chemical Society).

Electrodes and their modifications. In terms of electrochemical sensors, electrodes play an essential role in signal transduction from analyte solution to electrochemical read-out system. In literature, electrodes for electrochemical biosensing of DBPs can be classified into two main groups, metal and carbon electrodes. There are only few reported studies on electrochemical detection of DBPs using metal electrodes, which usually featured relatively simple electrode assembly without using either signal amplifications or recognition molecules. For example, Peverly et al. reported an electrolysis-deposition-stripping protocol on voltammetric determination of THMs in water by means of silver electrode[75]. Cetó et al. explored an 'electronic tongue' strategy by using voltammetric measurements and chemometric tools, such as principal component analysis (PCA) and artificial neural network (ANN) model, for electrochemical detection of HAAs (especially HAA3) on gold electrode[70]. Li et al. created a miniaturized electrochemical gold sensor integrated with polydimethylsiloxane (PDMS) microfluidic channels for the determination of DBA and TBM (shown in **Figure 3a**), showing an ultrasensitive detection level of 1 part per trillion (ppt)[71].

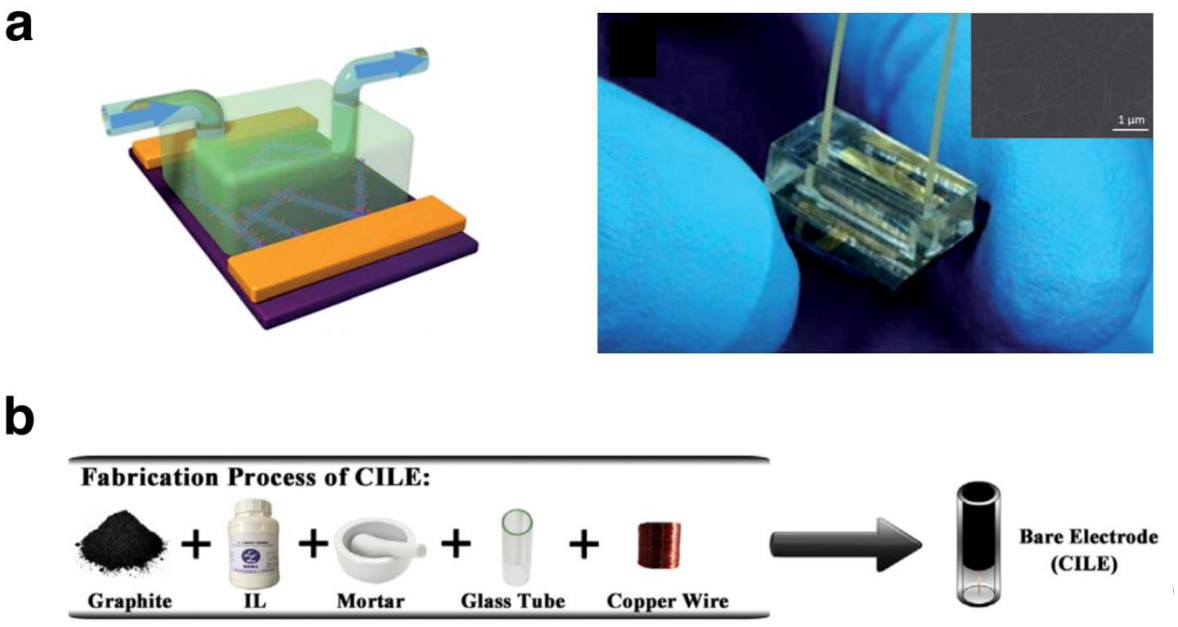

Figure 3. a. schematic and image of the miniaturized sensor integrated with a PDMS microchannel to form a solution flowing environment (Reproduced with permission of ref 71, Copyright 2017 Royal Society of Chemistry) and b. fabrication process of CILE (Reproduced with permission of ref 73, Copyright 2018 Elsevier).

Compared with metal electrodes, carbon materials (e.g. graphite) are more cost-effective and suitable for mass production due to their ubiquitous source. Therefore, they have been considered as more promising alternatives as electrode materials and received far more attention in electrochemical detection of DBPs (see **Table 2**). In reported literature, glassy carbon electrode (GCE)[36,37,38,42,61,72,76] and carbon paste electrode (CPE)[43] are examples of carbon electrodes. Between them, an improved version of CPE, such as carbon ionic liquid electrode (CILE), has been developed and utilized as it is a strong preference for electrochemical sensors[39,40,41,42,44,45,46,47,48,50,51,52,53,54,55,56,57,58,59,60,62,63,64,65,66,67,68,73,74] owing to less electrode fouling and better electron transfer kinetics[40]. It can be easily fabricated through a homogenous blending of graphite powder and ionic liquid (IL), which was then loaded into a glass tube with a copper wire throughout the bulk to establish an electrical contact[37]. A typical procedure is

schematically presented in **Figure 3b**. Several ILs have been reported in the fabrication of CILE, including N-hexylpyridinium hexafluorophosphate ($HPPF_6$)[40,45,46,47,50,51,52,55,56,57,58,59,62,65,66,67,68,73], 1-butylpyridinium hexafluorophosphate ($BPPF_6$)[44,48,53,54], 1-(3-chloro-2-hydroxyl-propyl)pyridinium tetrafluoroborate ($PPBF_4$)[41], 1-butyl-3-methylimidazolium tetrafluoroborate ($BMIMBF_4$)[60] and 1-ethyl-3-methylimidazolium tetrafluoroborate ($EMIMBF_4$)[63].

In general, DBPs detection using unmodified carbon electrodes cannot achieve desirable analytical level due to poor signal stability, unfavorable reproducibility, tardy electrode kinetics with high over-potentials between target molecules and electrodes. More importantly, some electroactive centres (e.g. Fe^{III}/Fe^{II} in heme proteins) are more likely to be shielded by chaotic polypeptide chains, leaving a hindrance to the pathways of electron transfer despite the fact that over-potentials can be significantly lowered by these electrocatalytic redox couples[42]. To overcome this challenge, many signal amplifiers have been used to improve sensor sensitivity and conductivity. As the most promising derivative of graphite, graphene (GR) has been extensively applied in many studies depending on its versatile properties including outstanding electrical and thermal conductivity, ultra-strong mechanical strength and extremely high specific surface area due to the unique sp^2 hybridized carbon atoms that closely packed as two-dimensional honeycomb lattice[90]. The other strong candidate is quasi one-dimensional carbon nanotubes (CNT) structurally viewed as rolled up graphene nanosheets, which have also been reported as signal amplifiers for TCA detection[35,41]. In laboratory, GR is normally produced using two routes: one is conventional Hummers method[91] which graphite is firstly oxidized into graphene oxide (GO) and then chemically reduced. However, rigorous reacting conditions, nasty solvents with subsequent selection of appropriate reducer are often required during the whole synthesis process, causing experimental complexity and potential health hazard; the other method is electroreduction of GO based on potentiostatic strategy[39,47,51,52,55,58,67], which proved to be more effective due to its facile process and the involvement of less harsh reagents. A special type of three-dimensional GR (3D-GR) with interconnected porous structure (see **Figure 4**) was also utilized as signal amplifier for electrochemical detection of TCA[52,55,67]. Compared with pristine GR, 3D-GR have less degree of aggregation caused by the relatively intense π-π stacking and Van der Waals interactions. Consequently, experimental results using 3D-GR modified electrodes showed better performance as compared to that of GR due to larger surface area, good conductive pathway and mobility of charge carriers. Furthermore, one study attempted to combine advantages of both GR and CNT by building a three-dimensional GR-CNT hybrid composite decorated CILE for the determination of TCA. In that study, significant improvement in LoD to 15.3 μM (3σ) was observed [45]. Finally, it is also noteworthy that GR and CNT modified electrodes can offer an extra synergistic coupling effects (e.g. reduced overpotential) when using metal complexes as recognition molecules (e.g. porphyrins) due to strong π–π stacking force between them [36,42].

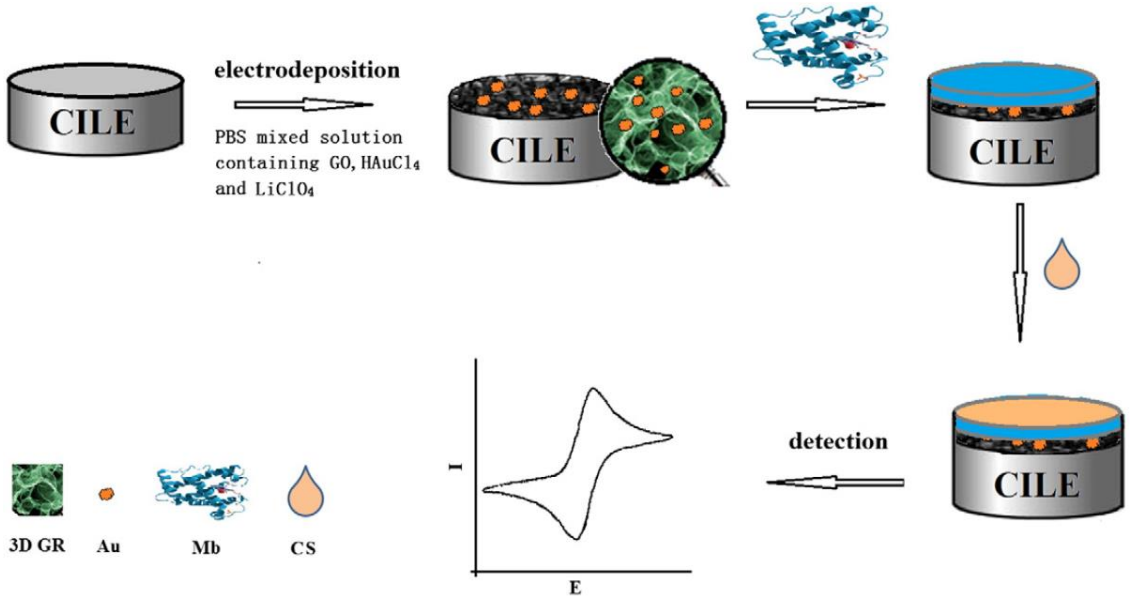

311 **Figure 4** The procedure of 3D-GR electrode fabrication and electrochemical detection (Reproduced with
312 permission of ref 55, Copyright 2016 Elsevier).

313 Furthermore, doping graphene with adjacent elements of similar atomic radius to carbon atom, such as
314 either boron (B) or nitrogen (N), has also been proposed for the modification of DBP sensor electrodes.
315 A nitrogen-doped graphene (NG) with Hb modified CILE for direct electrocatalytic reduction toward
316 TCA was demonstrated by Sun et al[50]. Graphitic carbon nitride (g-C_3N_4) was employed by Zhan et al.
317 due to its excellent thermal stability, dense inner plane nitrogen content and favorable electronic
318 structure[74]. Chen at al. performed a highly similar experiment that applied boron-doped graphene
319 quantum dots (B-GQDs) with Hb decorated CILE to accomplish voltammetric measurements of the
320 same target[73]. Interestingly, electrochemical results shown by the latter demonstrated remarkably wider
321 detection range and LoD, which was an order of magnitude lower than that of the former. This
322 phenomenon is probably ascribed to dopant B atom, which is electron-deficient and lack one electron
323 from outermost layer as compared to carbon atom, thus enhancing the electronic properties (e.g.
324 conductivity) of the GQDs[73].

325 Some studies suggested that signal amplifiers (e.g. GR) could form a synergistic effect with electrode
326 additives such as IL and layered double hydroxide (LDH) to promote electron transfer. As a matter of
327 fact, IL is not only ingredient of CILE, but also utilized as a binder and disperser to prevent GR from
328 self-agglomeration depending on its special composites of a small anion with a huge cation like
329 imidazolium or pyridinium[36,40,60,63,64]. LDH is a special sheet-shaped aquo-complex that has large
330 surface area, good biocompatibility and diverse chemical properties due to different metallic
331 compositions such as Mg_2Al[46] and Co_2Al[54,74]. Layer charge density can be changed easily because of
332 its extraordinary ion-exchange abilities, indicating a broad application prospect in electrochemical
333 biosensing. Nevertheless, the sensor performances were not significantly improved by this synergy due
334 to the fact that most of detection ranges and LoDs were as high as mM level from the results of
335 electrochemical detection. Such inconsistency could be caused by inappropriate selection of buffer
336 solution (e.g. unsuitable pH) affecting the efficiency of electron transfer. Both IL and LDH are positive
337 charged compounds that prefer to conjugate with negative charged biological macromolecules. On the
338 other hand, proteins especially made up of amphoteric amino acids can be either positive or negative.

Therefore, the pH value between buffer solution and isoelectric point should be reasonably controlled to ensure less resistance for electron transfer.

To further improve the electron transfer and biocompatibility of electrochemical biosensors, metal nanoparticles (e.g. AuNPs[47,55], AgNPs[39], PtNPs[48] and PdNPs[62]), films (e.g. Bi film[58]), metal oxides or sulfide (e.g. TiO_2[44], NiO[51,63], ZrO_2[57], Fe_3O_4[59], Co_3O_4[60], SnO_2[64], ZnO[67] and CuS[53]) were also introduced to graphene or CNT modified carbon electrodes as bridging materials with recognition molecules, such as redox proteins. As a result, electrodes modified by the introduction of metal nanoparticles[38] or oxides[43] produced more sensitive sensors compared with electrode-metallic additive-redox protein assemblies. Bashami et al. developed a glass carbon electrode (GCE) modified with AgNPs and malic acid (MA) for electrochemical biosensing of TCA[72]. In their work, MA was used as a crosslinker and immobilizer for AgNPs through hydrogen bonding as well as electrostatic effect, which is shown in **Figure 5a**. Qian et al. constructed a core-shell Au@Ag nanorods (Ag@GNRs) (see **Figure 5b**) based sensor electrode with further modification of Hb, poly (diallyldimethylammonium chloride) (PDDA) and polystyrene sulfonate (PSS) for the determination of TCA. A broad detection range was obtained as well as significantly improved LoD from mM down to μM[61]. Dai et al. fabricated a new sensing interface by immobilizing the TiO_2 nanotubes (TNTs) with thionine onto GCE, which was reported to have a good biocompatibility and special reaction channel. Due to acceleration of the electron transmission rate and improved electrochemical behavior of thionine, a wider linear range for the detection of TCA was achieved between 6 μM and 1.5 mM[37].

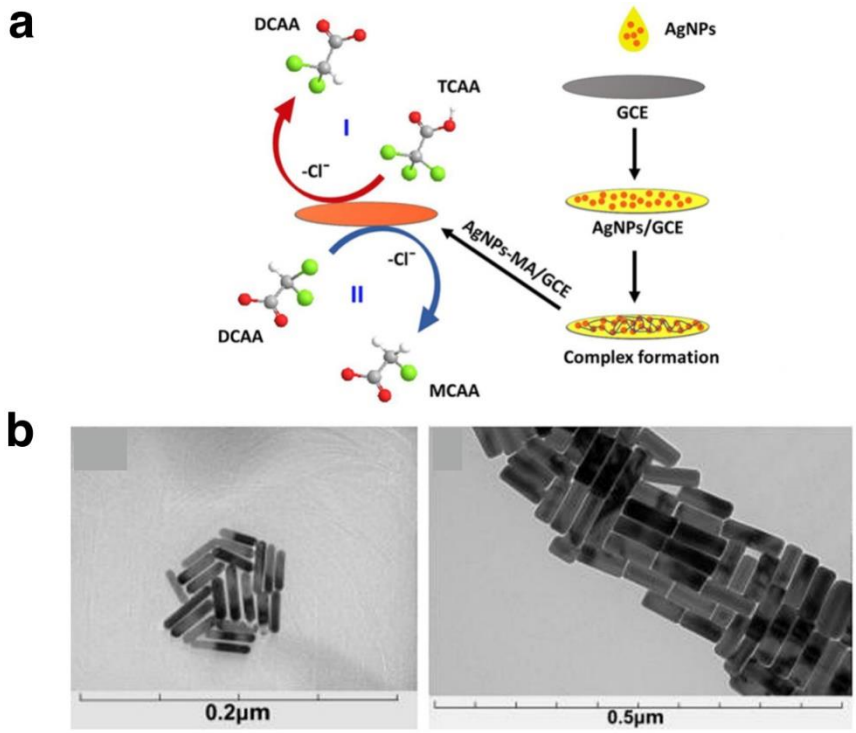

Figure 5. Preparation schematics of a. AgNPs-MA/GCE (Reproduced with permission from ref 72, Copyright 2018 Elsevier) and b. TEM spectra of left: gold nanorods (GNRs) and right: core-shell Ag@GNRs (Reproduced with permission of ref 61, Copyright 2017 Springer).

Electrochemical Detection Techniques. Data processing of electrochemical sensors normally undergoes three steps including signal capture, transformation and data acquisition. Techniques for electrochemical sensing detection can be interpreted as electrical representations in accordance with each moment of biochemical reacting in the analytical solution. In literature, electrochemical detection of DBP in water was mostly carried out using current-related monitoring techniques, such as amperometry, cyclic voltammetry (CV), differential pulse voltammetry (DPV), square wave voltammetry (SWV). Typical graphs of each technique are shown in **Figure 5**, respectively.

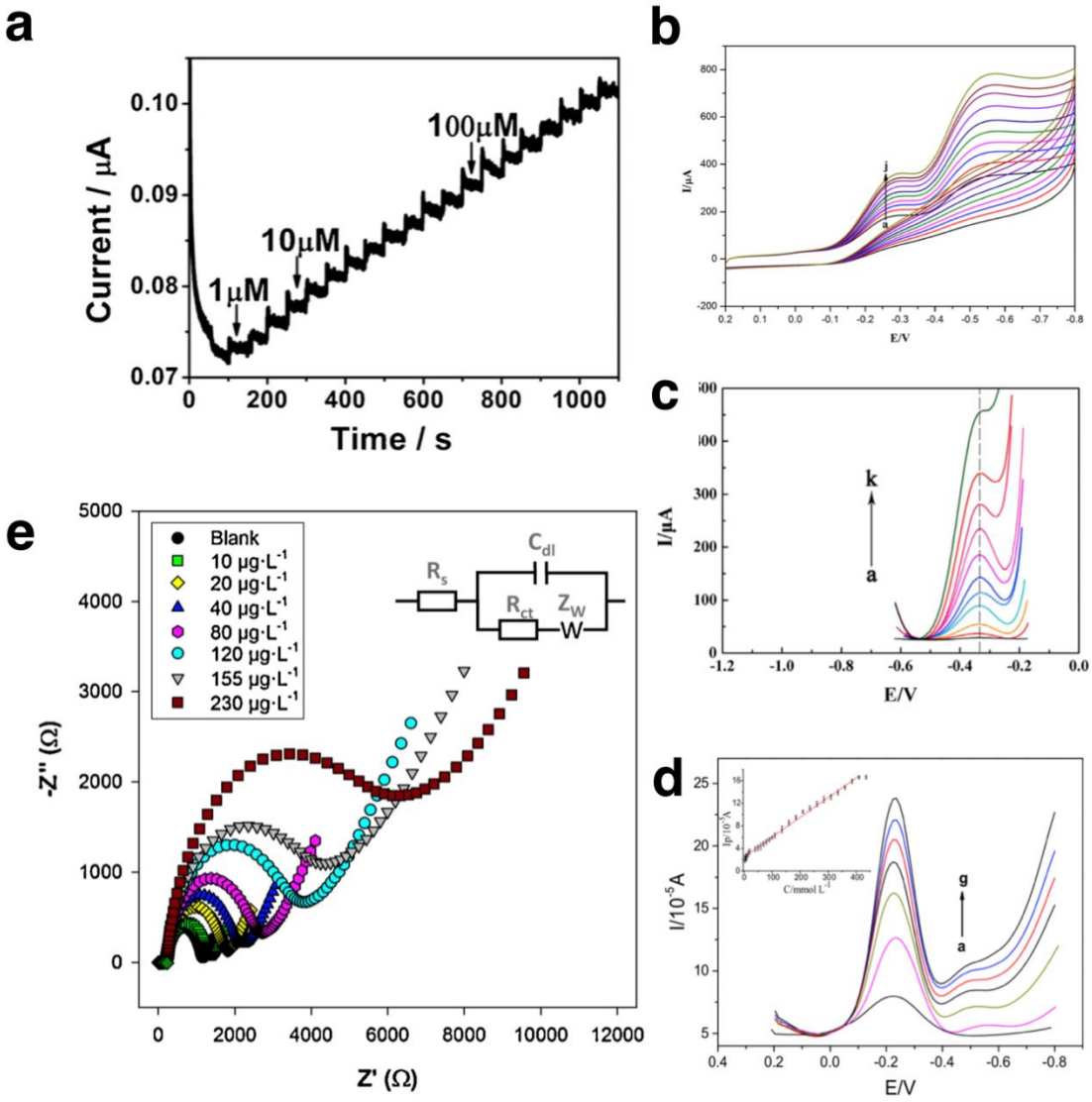

Figure 6. Different concentrations of DBPs detected using various of electrochemical techniques: a. Amperometry (Reproduced with permission of ref 61, Copyright 2017 Springer), b. CV (Reproduced with permission of ref 59, Copyright 2017 Springer), c. DPV (Reproduced with permission of ref 73, Copyright 2018 Elsevier), d. SWV (Reproduced with permission of ref 54, Copyright 2016 Elsevier), and e. EIS, where shows different concentrations of NDMA (Reproduced with permission of ref 76, Copyright 2016 Elsevier).

So far, CV is the most reported technique for electrochemical biosensing of DBPs as shown in **Table 2**. A typical cyclic voltammogram is obtained by measuring the current at the working electrode during multiple or single potential loop scans generally starting from reduction process with increasingly

negative potentials followed by a re-oxidation process caused by reversed potential scanning. Interestingly, no extra redox couple was required when applying CV as an electrochemical technique for the detection of DBP (e.g. TCA). This was mainly due to the involvement of enzymes (e.g. HRP) and heme proteins (e.g. Hb and Mb) that already have ferric/ferrous ion (Fe^{III}/Fe^{II}) in their molecular structure. When using heme proteins for electrochemical measurements of TCA, the reduction process occurs at the cathode and most of CV graphs have two reduction peak currents (see **Figure 6b**): 1) the first peak corresponds to the reduction of TCA to di- or mono-chloroacetic acid by the Fe^{II} reduced from Fe^{III} , and 2) the second peak signals a further dichlorination of di- or mono-chloroacetic acid to acetic acid with highly reduced form of Fe^{I} [39]. The oxidation peak also gradually disappeared, which was ascribed to the presence of Hb molecules on the electrode and their good catalytic ability to TCA. The peak currents for the cathodic reduction of TCA were found to be proportional to the square root of the scan rate in most studies, exhibiting a characteristic diffusion-controlled process of analyte as expected for a catalytic system. In addition, the reduction peak current of TCA usually levelled off to a plateau with the increase of TCA concentration, indicating a typical Michaelis-Menten kinetic mechanism[92]. This maximum detection values in literature varied between 10 and 300 mmol/L for TCA measurement[43, 63, 73]. On the other hand, it should be noted that CV is not particularly sensitive for low TCA concentrations, which was demonstrated by Kurd et al[42]. In their study, a good linear relationship was obtained between current and analyte concentration using amperometry especially in the region of low concentrations with much improved LoD as compared to CV measurements. Furthermore, Sun et al. showed an enlarged range of TCA detection using DPV compared with the same target measured by CV[46]. Chen et al. observed a similar enlargement of detection range when DPV measurements were applied[73]. Bashami et al. attempted to develop a background interference-eliminated analytical method for the electrochemical determination of TCA, in which reduction peak of TCA using SWV were most distinctive compared with CV and DPV under identical experimental conditions[72].

In addition to voltammetry or amperometry, impedance or resistance-related monitoring, such as electrochemical impedance spectroscopy (EIS), is another promising analytical technique for monitoring chemical or physical changes of electrode surface, which displays many advantages such as low cost, fast and stable response, ease of operation and high sensitivity. For EIS measurements, AC signals of different frequencies are applied between the electrodes while the voltage and current are monitored. This allows the frequency-dependent electrical parameters (e.g. charge transfer resistance and capacitance) to be measured. In most literature (as seen in **Table 2**), EIS was mainly applied in combination with scanning electron microscopy (SEM) images to characterize the electrode modification rather than used as a direct electrochemical biosensing technique for determination of DBPs. Electroactive redox probe (e.g. $[Fe(CN)_6]^{3-/4-}$) is often required when a faradaic EIS measurement is performed. Charge transfer resistance is closely dependent on the interaction between redox couple and the electrode, where functionalized electrode surface gives higher resistance compared with the one without any modification. For example, Cetó et al. demonstrated a MIP sensor for the electrochemical detection of NDMA using redox probe (e.g. 10 mM of $[Fe(CN)_6]^{3-/4-}$) assisted EIS measurements[76]. As shown in Figure 6e, charge transfer resistance was observed to increase linearly with NDMA concentration in obtained Nyquist plot, where semi-circle indicates charge transfer process and was highly distinctive even at very low concentrations. Li et al. developed functionalized DWCNTs biosensor for the detection of trace amount of brominated DBPs (e.g. DBA and TBM) [71]. The selectivity of the sensors towards DBA can be tuned by switching functional groups of the DWCNTs from

carboxyl to amino. Resistance, observed from the *I-V* curves, increased as more concentrated DBPs were introduced into the solution, showing a positive correlation between voltage and current. Kibechu et al. fabricated a MIP based chemo-sensor for the detection of TCA in aqueous solution by monitoring voltage drop on a homemade circuit initially applied with 5V[49]. The sensing signal after each introduction of TCA into the solution was stable for as long as 10s, although test on real drinking water sample and storage stability was lacking.

CURRENT CHALLENGES AND FUTURE RESEARCH DIRECTIONS

Early detection of DBPs formation requires sensitive, cost-effective, easy-to-use and high-throughput analytical techniques. However, current laboratory techniques (e.g. HPLC-MS) do not meet these requirements. Moreover, there is an ever-increasing list of DBPs that may be present in drinking water, increasing the need for cost-effective generic analysis platforms. These platforms should be easily tailored to provide early warnings of contamination episodes and should also allow screening for a wide range of key parameters in water quality from catchment to consumer. Despite the progress in the last decade, there are still some major challenges and thus opportunities in the research area of electrochemical sensing of DBPs in water, including the following:

1) So far electrochemical detection of TCA received the most attention. Similar research on NDMA is seriously lacking with only one paper published. Given the high-level toxicity of NDMA as DBP in drinking water, more research effort is required to develop electrochemical sensors for this target in order to close the gap.
2) The possible activity change of immobilized biological recognition molecules upon long-term storage affects the practicality of these biosensors. For most electrochemical sensors using redox proteins, metal complexes and enzymes as recognition molecules for TCA, film forming agents including hyulanonic acid, sodium alginate, chitosan and Nafion were deposited onto sensor electrodes (e.g. via electrodeposition) to create a protective microenvironment and minimise denaturation or leakage of biomolecules during the fabrication process. Various ionic liquids were also added as binders to enhance resistance against electrode-fouling, electron transfer rate, electrochemical stability and sensitivity[93,94, 95]. However, there is no systematic comparison study on the effectiveness of different polymeric film and ionic liquids.
3) In addition, no selectivity assessment against other similar DBP variants was carried out in any of the reported TCA sensors. This seriously limited the practical application of these biosensors since simultaneous generation of multiple DBP analogues are very common during any modern disinfection process. On that note, multiplex detection of similar DBP analogues are certainly desirable, which can for example be achieved by incorporating artificial neuron network (ANN) methods.
4) In recent decades, MIP technique has attracted increasing attentions in the field of electrochemical biosensing. Compared to biological recognition systems (e.g. redox proteins and enzymes mostly used in electrochemical detection of DBPs), well-known advantages of MIPs include low production cost, long shelve-life, re-usable without loss of selectivity, ease of preparation, high mechanical strength, high thermal and chemical stability. In addition, MIP technique can be particularly advantageous when combined with non-Faradaic EIS, which could potentially allow continuous in-situ monitoring since no electroactive redox species (e.g. Fe^{III}/Fe^{II}) are required in the analyte solution. In a typical non-Faradaic EIS measurement, phase offset or shift between the input voltage

and output current is commonly used as electrochemical sensing signal, which directly reflect any physical change (e.g. a recognition event) occurred on the electrode interface and that in interfacial capacitance[96,97]. EIS-based DBPs biosensor could be a powerful diagnostic tool, since non-faradaic EIS technique has been demonstrated for successful detection of different biomarkers for diseases, such as diabetes, cancer and cardiovascular diseases[98, 99, 100, 101]. For any successful non-faradaic EIS measurement, a full coverage of insulating self-assembly monolayer (SAM) on the surface of sensor electrodes is essential and need to be meticulously carried out.

5) For most of reported studies, response time of electrochemical biosensors for DBP detection was not widely reported and discussed. In general, 20 min or less in response time is highly desirable for any realistic in-situ monitoring or being commercially meaningful. Therefore, future effort of more systematic feasibility and comparison studies across different DBP sensor designs in terms of response time should be carried out to explore their full commercial potential.

ACKNOWLEDGEMENT

This work was partly funded by European Commission Horizon 2020 Marie Skłodowska-Curie Actions (Grant Agreement No.743993). Dr Wei Zhang would also like to acknowledge the support from Florence Mockeridge Fellowship Group, Swansea University.

VOCABULARY

Disinfection by-products (DBPs) can exist as wide variety of compounds, as result of the highly reactive nature of disinfectants interacting with natural organic matters in water sources; *N*-nitrosodimethylamine (NDMA) is an emerging DBP detected in water and currently classified as "probably carcinogenic to humans" by the International Agency for Research on Cancer; Electrochemical impedance spectroscopy (EIS), is a frequently used method for monitoring change of electrochemical response upon a bio-recognition event at an electrode surface with high sensitivity; Molecular imprinted polymers (MIP) are a novel group of synthetic bioreceptors with specially manufactured microcavities showing high affinity and specificity for any given analyte molecule; Self-assembled monolayers (SAM), is formed by the chemisorption of organic molecules onto a substrate from either the vapor or liquid phase followed by a slow and orderly organization into thin monolayer deposit.

REFERNCES

(1) Zhang, W.; Zhang, Y.; Fan, R.; Lewis, R. A facile TiO_2/PVDF composite membrane synthesis and their application in water purification. *J. Nanopart. Res.* **2016**, *18*, 31. DOI: 10.1007/s11051-015-3281-1

(2) Zhang, W.; Zou, L.; Wang, L. Visible-light assisted methylene blue (MB) removal by novel TiO_2/adsorbent nanocomposites. *Water Sci. Technol.* **2010**, *61*, 2863– 2871.

(3) José Farré, M.; Reungoat, J.; Argaud, F. X.; Ratter, M.; Keller, J.; Gernjak, W. Fate of N-nitrosodimethylamine, trihalomethane and haloacetic acid precursors in tertiary treatment including biofiltration, *Water Res.* **2011**, *45*, 5695-5704.

(4) Guidelines for Drinking-Water Quality, 4th ed. World Health Organization. ISBN 978-92-4-154995-0.

(5) Ghernaout, D.; Ghernaout, B. From chemical disinfection to electrodisinfection: The obligatory itinerary? *Desalin. Water Treat.* **2010**, *16*, 156-175.

(6) Richardson, S. D.; Postigo, C. (2011) Drinking water disinfection by-products. In *Emerging organic contaminants and human health* (pp. 93-137). Springer, Berlin, Heidelberg.

(7) Roberts, M. G.; Singer, P. C.; Obolensky, A. Comparing total HAA and total THM concentrations using ICR data. *J. Am. Water Works Assoc.* **2002**, *94*, 103-114.

(8) Plewa, M. J.; Simmons, J. E.; Richardson, S. D.; Wagner, E. D. Mammalian cell cytotoxicity and genotoxicity of the haloacetic acids, a major class of drinking water disinfection by- products. *Environ. Mol. Mutagen.* **2010**, *51*, 871-878.
(9) USEPA (US Environmental Protection Agency). National Primary Drinking Water Regulations: Stage 2 Disinfectants and Disinfection Byproducts Rule: Final Rule. *Fed. Reg.* **2006**, *71*, 387-493.
(10) Liu, B.; Hu, X.; Deng, Y.; Yang, S.; Sun, C. Selective determination of trichloroacetic acid using silver nanoparticle coated multi-walled carbon nanotubes. *Electrochem. Commun.* **2010**, *12*, 1395-1397.
(11) Parvez, S.; Rivera-Núñez, Z.; Meyer, A.; Wright, J. M. Temporal variability in trihalomethane and haloacetic acid concentrations in Massachusetts public drinking water systems. *Environ. Res.* **2011**, *111*, 499-509.
(12) Wright, J. M.; Schwartz, J.; Dockery, D. W. The effect of disinfection by-products and mutagenic activity on birth weight and gestational duration. *Environ. Health Perspect.* **2004**, *112*, 920-925.
(13) Uden, P. C.; Miller, J. W. Chlorinated acids and chloral in drinking water. *J. Am. Water Works Assoc.* **1983**, *75*, 524-527.
(14) Cape, N.; Forczek, S.; Gullner, G.; Mena-Benitez, G.; Schröder, P.; Matucha, M. Progress in Understanding the Sources, Deposition and Above-ground Fate of Trichloroacetic Acid (11 pp). *Environ. Sci. Pollut. Res.* **2006**, *13*, 276-286.
(15) Bhat, H. K.; Kanz, M. F.; Campbell, G. A.; Ansari, G. A. S. Ninety day toxicity study of chloroacetic acids in rats. *Toxicol. Sci.* **1991**, *17*, 240-253.
(16) Linder, R. E.; Klinefelter, G. K.; Strader, L. F.; Suarez, J. D.; Dyer, C. J. Acute spermatogenic effects of bromoacetic acids. *Toxicol. Sci.* **1994**, *22*, 422-430.
(17) Moser, V. C.; Phillips, P. M.; Levine, A. B.; McDaniel, K. L.; Sills, R. C.; Jortner, B. S.; Butt, M. T. Neurotoxicity produced by dibromoacetic acid in drinking water of rats. *Toxicol. Sci.* **2004**, *79*, 112-122.
(18) Plewa, M. J.; Wagner, E. D.; Muellner, M. G.; Hsu, K. M.; Richardson, S. D. Chapter 3 Comparative mammalian cell toxicity of N-DBPs and C-DBPs. *ACS Symposium Series: Disinfection By-Produces in Drinking Water* **2008**, *995*, 36-50.
(19) Plewa, M. J.; Kargalioglu, Y.; Vankerk, D.; Minear, R. A.; Wagner, E. D. Mammalian cell cytotoxicity and genotoxicity analysis of drinking water disinfection by- products. *Environ. Mol. Mutagen.* **2002**, *40*, 134-142.
(20) Richardson, S. D. Disinfection by-products and other emerging contaminants in drinking water. *TrAC Trends Anal. Chem.* **2003**, *22*, 666-684.
(21) Peverly, A. A.; Peters, D. G. Electrochemical determination of trihalomethanes in water by means of stripping analysis. *Anal. Chem.* **2012**, *84*, 6110-6115.
(22) Pourmoghaddas, H.; Stevens, A. A. Relationship between trihalomethanes and haloacetic acids with total organic halogen during chlorination. *Water Res.* **1995**, *29*, 2059-2062.
(23) Horth, H. Identification of mutagens in drinking water. *Aqua* **1989**, *38*, 80-100.
(24) Cappelletti, M.; Frascari, D.; Zannoni, D.; Fedi, S. Microbial degradation of chloroform. *Appl. Microbiol. Biotechnol.* **2012**, *96*, 1395-1409.
(25) Trihalomethanes in Drinking-water. Background document for development of WHO Guidelines for Drinking-water Quality.
(26) Public Health Statement for Bromoform and Dibromochloromethane.
(27) Palmer, C. J.; Reason, C. J. Relationships of surface bromoform concentrations with mixed layer depth and salinity in the tropical oceans. *Global Biogeochem. Cy.* **2009**, *23*, GB2014.
(28) José Farré, M.; Insa S.; Mamo, J.; Barceló, D. Determination of 15 N-nitrosodimethylamine precursors in different water matrices by automated on-line solid-phase extraction ultra-high-performance-liquid chromatography tandem mass spectrometry, *J. Chromatogr. A* **2016**, *1458*, 99–111.
(29) Dai, N.; Mitch, W. A. Relative importance of N-nitrosodimethylamine compared to total N-nitrosamines in drinking waters. *Environ. Sci. Technol.* **2013**, *47*, 3648-3656.
(30) Dai, N.; Zeng, T.; Mitch, W. A. Predicting N-nitrosamines: N-Nitrosodiethanolamine as a significant component of total N-nitrosamines in recycled wastewater. *Environ. Sci. Technol. Lett.* **2015**, *2*, 54-58.

(31) Sgroi, M.; Vagliasindi, F.; Snyder, S.; Roccaro, P. *N*-Nitrosodimethylamine (NDMA) and its precursors in water and wastewater: A review on formation and removal, *Chemosphere* **2018**, *191*, 685-703.
(32) Zhou, W. J.; Boyd, J. M.; Qin, F.; Hrudey, S. E.; Li, X. F. Formation of N-nitrosodiphenylamine and two new N-containing disinfection byproducts from chloramination of water containing diphenylamine. *Environ. Sci. Technol.* **2009**, *43*, 8443-8448.
(33) ATSDR (Agency for Toxic Substances and Disease Registry). 1989. Toxicological profile for *N*-nitrosodimethylamine. Prepared by the Syracuse Research Corporation for ATSDR in collaboration with the U.S. Environmental Protection Agency. U.S. Public Health Service, Washington, D.C. 119 pp.
(34) Mitch, W. A.; Sharp, J. O.; Trussell, R. R.; Valentine, R. L.; Alvarez-Cohen, L.; Sedlak, D. L. N-nitrosodimethylamine (NDMA) as a drinking water contaminant: a review. *Environ. Eng. Sci.* **2003**, *20*, 389-404.
(35) Li, X.; Mitch W.A. Drinking water disinfection byproducts (DBPs) and human health effects: Multidisciplinary challenges and opportunities, *Environ. Sci. Technol.* **2018**, *52*, 1681-1689.
(36) Tu, W.; Lei, J.; Ju, H. Functionalization of carbon nanotubes with water- insoluble porphyrin in ionic liquid: direct electrochemistry and highly sensitive amperometric biosensing for trichloroacetic acid. *Chem. Eur. J.* **2009**, *15*, 779-784.
(37) Dai, H.; Xu, H.; Wu, X.; Lin, Y.; Wei, M.; Chen, G. Electrochemical behavior of thionine at titanate nanotubes-based modified electrode: A sensing platform for the detection of trichloroacetic acid. *Talanta* **2010**, *81*, 1461-1466.
(38) Liu, B.; Deng, Y.; Hu, X.; Gao, Z.; Sun, C. Electrochemical sensing of trichloroacetic acid based on silver nanoparticles doped chitosan hydrogel film prepared with controllable electrodeposition. *Electrochim. Acta* **2012**, *76*, 410-415.
(39) Sun, W.; Zhang, Y.; Wang, X.; Ju, X.; Wang, D.; Wu, J.; Sun, Z. Electrodeposited graphene and silver nanoparticles modified electrode for direct electrochemistry and electrocatalysis of hemoglobin. *Electroanalysis* **2012**, *24*, 1973-1979.
(40) Ruan, C.; Li, T.; Niu, Q.; Lu, M.; Lou, J.; Gao, W.; Sun, W. Electrochemical myoglobin biosensor based on graphene–ionic liquid–chitosan bionanocomposites: Direct electrochemistry and electrocatalysis. *Electrochim. Acta* **2012**, *64*, 183-189.
(41) Sun, W.; Guo, Y.; Li, T.; Ju, X.; Lou, J.; Ruan, C. Electrochemistry of horseradish peroxidase entrapped in graphene and dsDNA composite modified carbon ionic liquid electrode. *Electrochim. Acta* **2012**, *75*, 381-386.
(42) Kurd, M.; Salimi, A.; Hallaj, R. Highly sensitive amperometric sensor for micromolar detection of trichloroacetic acid based on multiwalled carbon nanotubes and Fe (II)–phtalocyanine modified glassy carbon electrode. *Mater. Sci. Eng. C* **2013**, *33*, 1720-1726.
(43) Najafi, M.; Darabi, S.; Tadjarodi, A.; Imani, M. Determination of trichloroacetic acid (TCAA) using CdO nanoparticles modified carbon paste electrode. *Electroanalysis*, **2013**, *25*, 487-492.
(44) Sun, W.; Guo, Y.; Ju, X.; Zhang, Y.; Wang, X.; Sun, Z. Direct electrochemistry of hemoglobin on graphene and titanium dioxide nanorods composite modified electrode and its electrocatalysis. *Biosens. Bioelectron.* **2013**, *42*, 207-213.
(45) Sun, W.; Cao, L.; Deng, Y.; Gong, S.; Shi, F.; Li, G.; Sun, Z. Direct electrochemistry with enhanced electrocatalytic activity of hemoglobin in hybrid modified electrodes composed of graphene and multi-walled carbon nanotubes. *Anal. Chim. Acta*, **2013**, *781*, 41-47.
(46) Sun, W.; Guo, Y.; Lu, Y.; Hu, A.; Shi, F.; Li, T.; Sun, Z. Electrochemical biosensor based on graphene, Mg2Al layered double hydroxide and hemoglobin composite. *Electrochim. Acta*, **2013**, *91*, 130-136.
(47) Li, G.; Li, T.; Deng, Y.; Cheng, Y.; Shi, F.; Sun, W.; Sun, Z. Electrodeposited nanogold decorated graphene modified carbon ionic liquid electrode for the electrochemical myoglobin biosensor. *J. Solid State Electrochem.* **2013**, *17*, 2333-2340.
(48) Sun, W.; Li, L.; Lei, B.; Li, T.; Ju, X.; Wang, X.; Li, G.; Sun, Z. Fabrication of graphene–platinum nanocomposite for the direct electrochemistry and electrocatalysis of myoglobin. *Mater. Sci. Eng. C* **2013**, *33*, 1907-1913.
(49) Kibechu, R. W.; Mamo, M. A.; Msagati, T. A.; Sampath, S.; Mamba, B. B. Synthesis and application of reduced graphene oxide and molecularly imprinted polymers composite in chemo sensor for trichloroacetic acid detection in aqueous solution. *Phys. Chem. Earth* **2014**, *76*, 49-53.

(50) Sun, W.; Dong, L.; Deng, Y.; Yu, J.; Wang, W.; Zhu, Q. Application of N-doped graphene modified carbon ionic liquid electrode for direct electrochemistry of hemoglobin. *Mater. Sci. Eng. C*, **2014**, *39*, 86-91.
(51) Sun, W.; Gong, S.; Deng, Y.; Li, T.; Cheng, Y.; Wang, W.; Wang, L. Electrodeposited nickel oxide and graphene modified carbon ionic liquid electrode for electrochemical myglobin biosensor. *Thin Solid Films* **2014**, *562*, 653-658.
(52) Sun, W.; Hou, F.; Gong, S.; Han, L.; Wang, W.; Shi, F.; Xi, J.; Wang, X.; Li, G. Direct electrochemistry and electrocatalysis of hemoglobin on three-dimensional graphene modified carbon ionic liquid electrode. *Sens. Actuators. B Chem.* **2015**, *219*, 331-337.
(53) Shi, F.; Zheng, W.; Wang, W.; Hou, F.; Lei, B.; Sun, Z.; Sun, W. Application of graphene–copper sulfide nanocomposite modified electrode for electrochemistry and electrocatalysis of hemoglobin. *Biosens. Bioelectron.* **2015**, *64*, 131-137.
(54) Zhan, T.; Wang, X.; Li, X.; Song, Y.; Hou, W. Hemoglobin immobilized in exfoliated Co_2Al LDH-graphene nanocomposite film: Direct electrochemistry and electrocatalysis toward trichloroacetic acid. *Sens. Actuators B Chem.* **2016**, *228*, 101-108.
(55) Shi, F.; Xi, J.; Hou, F.; Han, L.; Li, G.; Gong, S.; Chen, C.; Sun, W. Application of three-dimensional reduced graphene oxide-gold composite modified electrode for direct electrochemistry and electrocatalysis of myoglobin. *Mater. Sci. Eng. C* **2016**, *58*, 450-457.
(56) Wang, W.; Li, X.; Yu, X.; Yan, L.; Shi, Z.; Wen, X.; Sun, W. Electrochemistry of multilayers of graphene and myoglobin modified electrode and its biosensing. *J. Chin. Chem. Soc.* **2016**, *63*, 298-302.
(57) Wang, W.; Li, X.; Yu, X.; Yan, L.; Lei, B.; Li, P.; Chen, C.; Sun, W. Electrochemistry and electrocatalysis of myoglobin on electrodeposited ZrO_2 and graphene-modified carbon ionic liquid electrode. *J. Iran. Chem. Soc.* **2016**, *13*, 323-330.
(58) Wang, X.; Liu, L.; Zheng, W.; Chen, W.; Li, G.; Sun, W. Electrochemical behaviors of myoglobin on graphene and Bi film modified electrode and electrocatalysis to trichloroacetic acid. *Int. J. Electrochem. Sci.* **2016**, *11*, 1821-1830.
(59) Chen, X.; Yan, H.; Shi, Z.; Feng, Y.; Li, J.; Lin, Q.; Wang, X.; Sun, W. A novel biosensor based on electro-co-deposition of sodium alginate-Fe_3O_4-graphene composite on the carbon ionic liquid electrode for the direct electrochemistry and electrocatalysis of myoglobin. *Polym. Bull.* **2017**, *74*, 75-90.
(60) Kang, S.; Zhao, W.; Li, X.; Wen, Z.; Niu, X.; He, B.; Li, L.; Sun, W. Electrochemical behaviors of myoglobin on ionic liquid-graphene-cobalt oxide nanoflower composite modified electrode and its electrocatalytic activity. *Inter. J. Electrochem. Sci.* **2017**, *12*, 2184-2193.
(61) Qian, D.; Li, W.; Chen, F.; Huang, Y.; Bao, N.; Gu, H.; Yu, C. Voltammetric sensor for trichloroacetic acid using a glassy carbon electrode modified with Au@ Ag nanorods and hemoglobin. *Microchim. Acta*, **2017**, *184*, 1977-1985.
(62) Chen, W.; Niu, X.; Li, X.; Li, X.; Li, G.; He, B.; Li, O.; Sun, W. Investigation on direct electrochemical and electrocatalytic behavior of hemoglobin on palladium-graphene modified electrode. *Mater. Sci. Eng. C* **2017**, *80*, 135-140.
(63) Zhao, W.; Li, X.; Wen, Z.; Niu, X.; Shen, Q.; Sun, Z.; Dong, R.; Sun, W. Application of ionic liquid-graphene-NiO hollowsphere composite modified electrode for electrochemical investigation on hemoglobin and electrocatalysis to trichloroacetic acid. *Inter. J. Electrochem. Sci.* **2017**, *12*, 4025-4034.
(64) Kong, L.; Du, Z.; Xie, Z.; Chen, R.; Jia, S.; Dong, R.; Sun, Z.; Sun, W. Electrochemistry of hemoglobin-ionic liquid-graphene-SnO_2 nanosheet composite modified electrode and electrocatalysis. *Inter. J. Electrochem. Sci.* **2017**, *12*, 2297-2305.
(65) Chen, X.; Feng, M.; Yan, H.; Sun, W.; Shi, Z.; Lin, Q. Fabrication of myoglobin-sodium alginate-graphene composite modified carbon ionic liquid electrode via the electrodeposition method and its electrocatalysis toward trichloroacetic acid. *Inter. J. Electrochem. Sci.* **2017**, *12*, 11633-11645.
(66) Zheng, W.; Zhao, W.; Chen, W.; Weng, W.; Liao, Z.; Dong, R.; Li, G.; Sun, W. Effect of carboxyl graphene on direct electrochemistry of myoglobin and electrocatalytic investigation. *Inter. J. Electrochem. Sci.* **2017**, *12*, 4341-4350.
(67) Wen, Z.; Zhao, W.; Li, X.; Niu, X.; Wang, X.; Yan, L.; Zhang, X.; Li, G.; Sun, W. Electrodeposited ZnO@three-dimensional graphene composite modified electrode for electrochemistry and electrocatalysis of myoglobin. *Inter. J. Electrochem. Sci.* **2017**, *12*, 2306-2314.

(68) Zheng, W.; Chen, W.; Weng, W.; Liu, L.; Li, G.; Wang, J.; Sun, W. Direct electron transfer of horseradish peroxidase at Co_3O_4–graphene nanocomposite modified electrode and electrocatalysis. *J. Iran. Chem. Soc.* **2017**, *14*, 925-932.
(69) Zhu, Z.; Li, Xia.; Wang, Y.; Zeng, Y.; Sun, W.; Huang, X. Direct electrochemistry and electrocatalysis of horseradish peroxidase with hyaluronic acid–ionic liquid–cadmium sulfide nanorod composite material. *Anal. Chim. Acta* **2010**, *670*, 51-56.
(70) Cetó, X.; Saint, C.; Chow, C. W.; Voelcker, N. H.; Prieto-Simón, B. Electrochemical fingerprints of brominated trihaloacetic acids (HAA3) mixtures in water. *Sens. Actuators B Chem.* **2017**, *247*, 70-77.
(71) Li, Z.; Yu, M.; Chu, Y.; Wu, X.; Huang, J.; Tao, W. 1 part per trillion level detection of disinfection byproducts in drinking water using miniaturized sensor. *J. Mater. Chem. A*, **2017**, *5*, 4842-4849.
(72) Bashami, R. M.; Soomro, M. T.; Khan, A. N.; Aazam, E. S.; Ismail, I. M.; El-Shahawi, M. S. A highly conductive thin film composite based on silver nanoparticles and malic acid for selective electrochemical sensing of trichloroacetic acid. *Anal. Chim Acta*, **2018**, *1036*, 33-48.
(73) Chen, W.; Weng, W.; Niu, X.; Li, X.; Men, Y.; Sun, W.; Li, G.; Dong, L. Boron-doped Graphene quantum dots modified electrode for electrochemistry and electrocatalysis of hemoglobin. *J. Electroanal. Chem.* **2018**, *823*, 137-145.
(74) Zhan, T.; Tan, Z.; Wang, X.; Hou, W. Hemoglobin immobilized in g-C_3N_4 nanoparticle decorated 3D graphene-LDH network: Direct electrochemistry and electrocatalysis to trichloroacetic acid. *Sens. Actuators B Chem.* **2018**, *255*, 149-158.
(75) Peverly, A. A.; Peters, D. G. Electrochemical determination of trihalomethanes in water by means of stripping analysis. *Anal. Chem.* **2012**, *84*, 6110-6115.
(76) Cetó, X.; Saint, C. P.; Chow, C. W.; Voelcker, N. H.; Prieto-Simón, B. Electrochemical detection of N- nitrosodimethylamine using a molecular imprinted polymer. *Sens. Actuators B Chem.* **2016**, *237*, 613-620.
(77) Zhang, W.; Jia, B.; Furumai, H. Fabrication of graphene film composite electrochemical biosensor as a pre-screening algal toxin detection tool in the event of water contamination. *Sci. Rep.* **2018**, *8* (10), 10686. DOI: 10.1038/s41598-018-28959-w
(78) Zhang, W.; Han, C.; Jia, B.; Saint, C.; Nadagouda, M.; Falaras, P.; Sygellou, L.; Vogiazi, V.; Dionysiou, D. A 3D graphene-based biosensor as an early microcystin-LR screening tool in sources of drinking water supply. *Electrochim. Acta* **2017**, *236*, 319– 327.
(79) Hernandez-Vargas, G.; Sosa-Hernández, J.; Saldarriaga-Hernandez, S.; Villalba-Rodríguez, A.; Parra-Saldivar, R.; Iqbal, H. Electrochemical biosensors: a solution to pollution detection with reference to environmental contaminants. *Biosensors* **2018**, *8*, 29. DOI: 10.3390/bios8020029
(80) Zhang, W.; Dixon, M. B.; C. Saint, C.; Teng, K. S.; Furumai, H. Electrochemical biosensing of algal toxins in water: The current state-of-art? *ACS Sens.* **2018**, *3*, 1233-1245.
(81) Jorge S. E.; Ribeiro D. M.; Santos M. N. N.; Sonati M. D. F. (2016) Hemoglobin: Structure, Synthesis and Oxygen Transport, Sickle Cell Anemia, Springer International Publishing.
(82) Suprun, E. V.; Shumyantseva, V. V.; Archakov, A. I. Protein electrochemistry: application in medicine. A review. *Electrochim. Acta*, **2014**, *140*, 72-82.
(83) Veitch, N. C. Horseradish peroxidase: a modern view of a classic enzyme. *Phytochemistry* **2004**, *65*, 249-259.
(84) Freeman, I.; Kedem, A.; Cohen, S. The effect of sulfation of alginate hydrogels on the specific binding and controlled release of heparin-binding proteins. *Biomaterials* **2008**, *29*, 3260-3268.
(85) Ding, C.; Zhang, M.; Zhao, F.; Zhang, S. Disposable biosensor and biocatalysis of horseradish peroxidase based on sodium alginate film and room temperature ionic liquid. *Anal. Biochem.* **2008**, *378*, 32-37.
(86) Cheong, M.; Zhitomirsky, I. Electrodeposition of alginic acid and composite films. *Colloids Surf. A Physicochem. Eng. Asp.* **2008**, *328*, 73-78.
(87) Najafi, M.; Mollazadeh, M. Selective recognition of chloroacetic acids by imprinted polyaniline film. *J. Appl. Polym. Sci.* **2011**, *121*, 292-298.
(88) Wulff, G. Molecular imprinting in cross- linked materials with the aid of molecular templates—a way towards artificial antibodies. *Angew. Chem. Inter. Ed.* **1995**, *34*, 1812-1832.

(89) Eersels, K.; Lieberzeit, P.; Wagner, P. A review on synthetic receptors for bioparticle detection created by surface-imprinting techniques-from principles to applications. *ACS Sens.* **2016**, *1*, 1171–1187.
(90) Bianco, A.; Cheng, H. M.; Enoki, T.; Gogotsi, Y.; Hurt, R. H.; Koratkar, N.; Kyotani, T.; Monthioux, M.; Park, C. R.; Tascon, J. M. D.; Zhang, J. All in the graphene family–a recommended nomenclature for two-dimensional carbon materials. *Carbon* **2013**, *65*, 1-6.
(91) Hummers Jr, W. S.; Offeman, R. E. Preparation of graphitic oxide. *J. Am. Chem. Soc.* **1958**, *80*, 1339-1339.
(92) Kamin, R. A.; Wilson, G. S. Rotating ring-disk enzyme electrode for biocatalysis kinetic studies and characterization of the immobilized enzyme layer. *Anal. Chem.* **1980**, *52*, 1198-1205.
(93) Zhan, T.; Guo, Y.; Xu, L.; Zhang, W.; Sun, W.; Hou, W. Electrochemistry and electrocatalysis of myoglobin intercalated in Mg_2Al-Cl layered double hydroxide and ionic liquid composite material, Talanta **2012**, *94*, 189–194.
(94) Sun, W.; Guo, Y.; Ju, X.; Zhang, Y.; Wang, X.; Sun, Z. Direct electrochemistry of hemoglobin on graphene and titanium dioxide nanorods composite modified electrode and its electrocatalysis, *Biosens. Bioelectron.* **2013**, *42*, 207–213.
(95) Wang, X.; Hao, J. Recent advances in ionic liquid-based electrochemical biosensors, *Sci. Bull.* **2016**, *61*, 1281-1295.
(96) Cai, X.; Baldelli, S. Surface barrier properties of self-assembly monolayers as deduced by sum frequency generation spectroscopy and electrochemistry. *J. Phys. Chem. C* **2011**, *115*, 19178-19189.
(97) Boubour, E.; Bruce Lennox, R. Insulating properties of self-assembled monolayers monitored by impedance spectroscopy. *Langmuir* **2000**, *16*, 4222-4228.
(98) Luo, X. L.; Xu, M. Y.; Freeman, C.; James, T.; Davis, J. J. Ultrasensitive Label Free Electrical Detection of Insulin in Neat Blood Serum. *Anal. Chem.* **2013**, *85* (8), 4129-4134.
(99) Jacobs, M.; Selvam, A. P.; Craven, J. E.; Prasad, S. Antibody-conjugated gold nanoparticle based immunosensor for ultra-sensitive detection of troponin-T. *J. Lab. Autom.* **2014**, *19* (6), 546-554.
(100) Jacobs, M.; Muthukumar, S.; Selvam, A. P.; Craven, J. E.; Prasad, S. Ultra-sensitive electrical immunoassay biosensors using nanotextured zinc oxide thin films on printed circuit board platforms. *Biosens. Bioelectron.* **2014**, *55*, 7-13.
(101) Assaifan, A. K.; Lloyd, J. S.; Samavat, S. Deganello, D.; Stanton, R. J.; Teng, K. S. Nanotextured surface on flexographic printed ZnO thin films for low-cost noon-faradaic biosensors. *ACS Appl. Mater. Interfaces* **2016**, *8*, 33802-33810.

For TOC Only

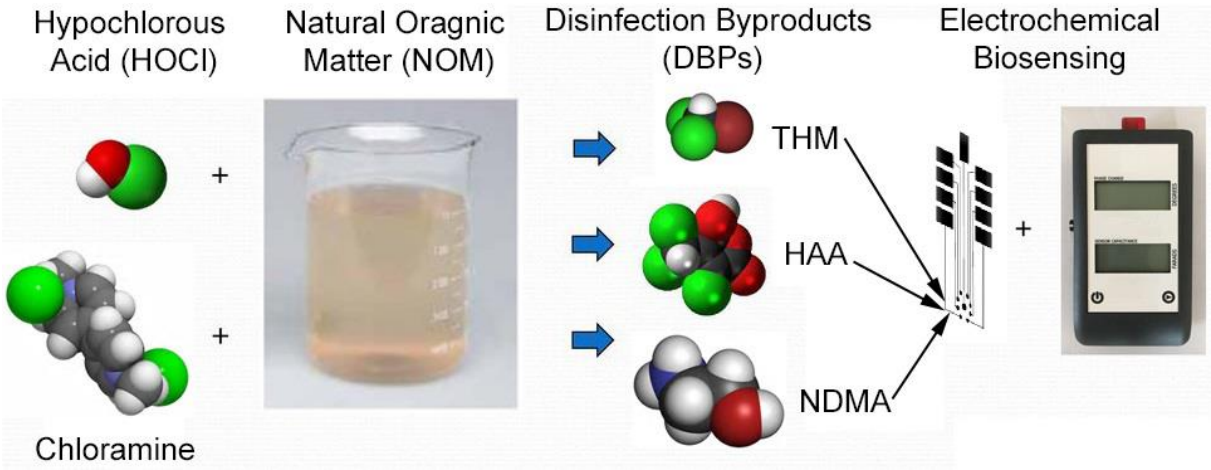
Hypochlorous Acid (HOCl)
Natural Oragnic Matter (NOM)
Disinfection Byproducts (DBPs)
Electrochemical Biosensing
+
+
Chloramine
THM
HAA
NDMA
+